

Article

A Numerical Analysis of the Role of Pile Foundations in Shaft Sinking Using the Vertical Shaft Sinking Machine (VSM)

Tianjun Liu ^{1,2}, Zongyu Liu ^{1,*} , Chunjing Ma ¹ , Zhibing Xu ³, Long Yu ³, Xu Zhang ³ and Keqi Liu ⁴ 

¹ Guangzhou Municipal Engineering Group Co., Ltd., Guangzhou 510060, China; liutianjun79@163.com (T.L.); machunjinglw@163.com (C.M.)

² Guangzhou Municipal Construction Group Co., Ltd., Guangzhou 510060, China

³ Shanghai Tunnel Engineering Rail Transit Design and Research Institute, Shanghai 200235, China; xu.zhibing@stedi.com.cn (Z.X.); yu.long@stedi.com.cn (L.Y.); zhang.xu@stedi.com.cn (X.Z.)

⁴ School of Resources and Civil Engineering, Northeastern University, Shenyang 110819, China; liukeqi@mail.neu.edu.cn

* Correspondence: zongyu.yyy@gmail.com

Abstract: The use of the Vertical Shaft Sinking Machine (VSM) for shaft construction marks a significant advancement in modern technology and is recognized as one of the leading techniques in the field. However, much of the existing research focuses on mechanical and technical challenges, often overlooking the effects on surrounding soil and the structural integrity of shafts. This study demonstrates that increasing pile diameter by 20% improves load-bearing capacity by 15% and reduces soil settlement by 12%, though these improvements come with higher construction costs. Additionally, larger diameters improve lateral stability, but excessively long piles lead to diminishing returns. To address the limited research on reinforcement design in soft soils, a series of numerical models were employed to investigate the effects of pile spacing, length, and diameter on surrounding soil behavior. This in-depth analysis aims to provide a scientific foundation for optimizing VSM technology in caisson pile foundations, particularly in soft-soil conditions.

Keywords: vertical shaft sinking machine; underground parking garage; pile foundation; structural design; numerical simulation



Citation: Liu, T.; Liu, Z.; Ma, C.; Xu, Z.; Yu, L.; Zhang, X.; Liu, K. A Numerical Analysis of the Role of Pile Foundations in Shaft Sinking Using the Vertical Shaft Sinking Machine (VSM). *Buildings* **2024**, *14*, 3383. <https://doi.org/10.3390/buildings14113383>

Academic Editor: Eugeniusz Koda

Received: 26 September 2024

Revised: 18 October 2024

Accepted: 21 October 2024

Published: 24 October 2024



Copyright: © 2024 by the authors. Licensee MDPI, Basel, Switzerland. This article is an open access article distributed under the terms and conditions of the Creative Commons Attribution (CC BY) license (<https://creativecommons.org/licenses/by/4.0/>).

1. Introduction

With the rapid growth of the global economy and the acceleration of urbanization, the prevalence of private vehicles has significantly increased, becoming an integral part of daily life for many households [1,2]. However, this surge in vehicle ownership has exacerbated parking challenges, particularly in densely populated urban areas [3]. The scarcity of urban land coupled with the rising demand for parking has driven urban planners and engineers to seek more efficient parking solutions. Underground parking garages, which can effectively alleviate urban traffic pressure without disrupting existing surface structures, have emerged as a vital component of modern urban infrastructure [4,5].

In the construction of underground parking facilities, the application of shaft structures has gained increasing attention [6]. These structures not only minimize ground-level disruption but also reduce the space required for construction sites and offer cost-effective solutions [7]. Traditionally, the construction of underground shafts, particularly for caisson foundations, has employed methods such as gravity caissons and pneumatic caissons, each with its own advantages and limitations.

Gravity caissons, also known as open caissons, are structures that sink into the ground due to their own weight. This method relies on excavation beneath the caisson, allowing it to gradually settle as soil is removed [8–10]. While effective for shallow depths, gravity caissons face significant challenges when sinking deeper shafts due to increased frictional

resistance between the caisson wall and surrounding soil. The friction often leads to uneven sinking and potential structural instability, particularly in heterogeneous soil conditions.

To mitigate these issues, the pneumatic caisson method was developed, where the caisson is pressurized with air, reducing the water and allowing for dry working conditions at significant depths. This method enables construction at depths exceeding 200 m, particularly in waterlogged or loose-soil environments. However, pneumatic caissons are highly complex, requiring sophisticated air compression systems, and their application is limited by the difficulty of maintaining consistent air pressure and controlling the rate of sinking [11,12].

To address some of these challenges, engineers turned to alternative methods, such as the use of bentonite or mud as a friction-reducing agent between caisson walls and the surrounding soil. This technique, popularized in the mid-20th century, involves injecting bentonite slurry between the caisson and soil to reduce friction, making it easier to sink the caisson. This method, although more effective than traditional gravity caissons, still encounters limitations related to soil heterogeneity and the difficulty of managing deep shaft excavation [13].

The introduction of the Super Open Caisson System (SOCS) in 1996 marked a significant advancement in the sinking of deep shafts [14]. The SOCS method combines underwater excavation techniques with advanced stabilization mechanisms. It utilizes specialized machinery, such as underwater excavators and mud pumps, to remove soil from beneath the caisson while grab buckets eliminate silt and other debris. In addition, ground anchors are employed to stabilize the shaft, providing resistance to sudden movements during excavation. The SOCS method has proven to be effective in controlling the sinking process, ensuring safety and stability at greater depths.

Among the most revolutionary innovations in shaft sinking technology is the Vertical Shaft Sinking Machine (VSM), developed by the German company Herrenknecht [15]. Unlike traditional methods, the VSM integrates mechanical excavation with precise control systems. The VSM uses cutting tools to excavate soil, which is then mixed with water and pumped out of the shaft. The shaft wall is constructed incrementally as the structure sinks, and a lowering device is employed to control the speed and stability of the shaft's descent. The VSM significantly reduces the risk of sudden sinking, a common issue in traditional caisson methods, by offering controlled excavation and shaft lowering, thus enhancing both safety and efficiency [16]. Furthermore, the mechanized nature of the VSM minimizes the environmental impact typically associated with conventional excavation methods, such as noise and vibrations.

However, despite these technological advancements, the application of VSM in real-world projects remains limited, especially in soft-soil conditions where settlement and shaft stability are more difficult to control. Current research on VSM technology is largely theoretical, and much of the design and implementation still relies on empirical engineering judgments. This lack of standardization has hindered the broader adoption of VSM technology in large-scale urban projects. Additionally, there is a critical gap in understanding the interaction between pile foundations and shaft stability during the sinking process, particularly in soft ground where shaft deformation and settlement risks are higher.

Beyond the VSM, other advanced caisson technologies have been developed, such as the Floating Caisson Method, where the caisson is prefabricated and floated to its final location before being sunk. This technique is primarily used in marine environments and offers an efficient way to build deep shafts without the need for extensive excavation machinery. However, its application is limited to specific environmental conditions and is not widely adopted in urban settings [11].

To address the gaps in research and practical application, this study focuses on the use of VSM technology in an underground parking garage project in Jing'an District, Shanghai, China. We investigate the interaction between the pile foundation and the shaft structure under different construction parameters. Based on comprehensive geotechnical tests and empirical data, soil parameters were determined, and finite difference software

FLAC^{3D} was used to simulate the mechanical behavior of the caisson structure under various conditions [17–19]. Previous studies such as Sun and Li (2022) [17] and Lei et al. (2023) [19] have demonstrated the effectiveness of FLAC^{3D} in simulating complex soil–structure interactions, particularly in deep foundation projects. Building upon these studies, this study aims to provide new insights into the behavior of pile foundations during the VSM construction process, contributing to the standardization and broader adoption of VSM technology in urban underground construction.

This study provides a detailed analysis of the construction process and critically evaluates the impact of pile foundation design on shaft stability. The findings demonstrate that optimizing pile parameters, such as diameter, spacing, and length, significantly improves load distribution and reduces soil settlement. By examining the interaction between the shaft and surrounding soil, this study offers practical guidance for the application of VSM technology and promotes safer and more efficient underground construction practices.

2. Methods: Application of VSM in Project Using Simulation

This section will introduce VSM technology and its specific application in the underground parking project in Jing'an District, Shanghai. It outlines the process of numerical modeling based on a fundamental description of the working conditions and the results of geological investigations. The modeling design is tailored to incorporate the specific construction characteristics and structural features of the VSM (Vertical Shaft Machine) used in the caisson construction process.

The numerical simulation is conducted using the Lagrangian finite difference geotechnical analysis software, FLAC^{3D}. This software is equipped with various built-in element types and constitutive models, enabling it to closely replicate real-world structural behaviors. FLAC^{3D} employs an explicit Lagrangian algorithm and a mixed discrete-partitioning technique, allowing for highly accurate simulations of material plastic failure and flow. These features make it ideal for modeling complex geotechnical processes, such as those encountered in the construction of deep shafts using VSM technology.

The numerical model consists of 111,688 solid elements, with 11 piles simulated using pile elements (a total of 372 structural elements). The hydraulic behavior is modeled using an isotropic seepage model, where the water flow in the soil conforms to Darcy's law.

2.1. Project Overview

The underground parking garage in Jing'an District of Shanghai is planned to be constructed using two caisson shafts, each with a diameter of 23.02 m and a depth of approximately 50.5 m, with a bottom buried depth of 44 m. The two caisson floors will cover an area of 286 square meters and will have a total of eight vehicle entrances and control rooms. The underground area covers 836 square meters and consists of a total of 19 floors, including equipment storage and a buried substation on the underground floor, as well as steel structure parking layers on the second floor and below, providing a total capacity for 304 parking spaces.

2.2. Geological and Hydrological Conditions

The geological conditions at the site are characterized by the following primary soil layers: mixed fill, clay silt, silty clay, muddy clay, silty clay interspersed with sandy silt, and interbedded silty clay and clay silt. The layers intersected by the shaft casing consist of various filling materials, with a thickness of approximately 2.73 m of mixed fill, 3.3 m of clay silt, 10.2 m of muddy clay, 26.3 m of silty clay, 6.6 m of silty clay interspersed with sandy silt, and a 7.5 m intercalated layer between the silty clay and clay silt. Beneath the bottom of the shaft, the area is predominantly composed of silt and fine sand, indicating that all excavated soil layers are classified as soft-soil layers.

The groundwater level is at a depth of -1 m, and the water level inside the shaft is consistent with the groundwater level.

2.3. Functional Principle of VSM

As shown in Figure 1, the arrangement of the equipment required for the VSM construction method in the project can be observed [16]:

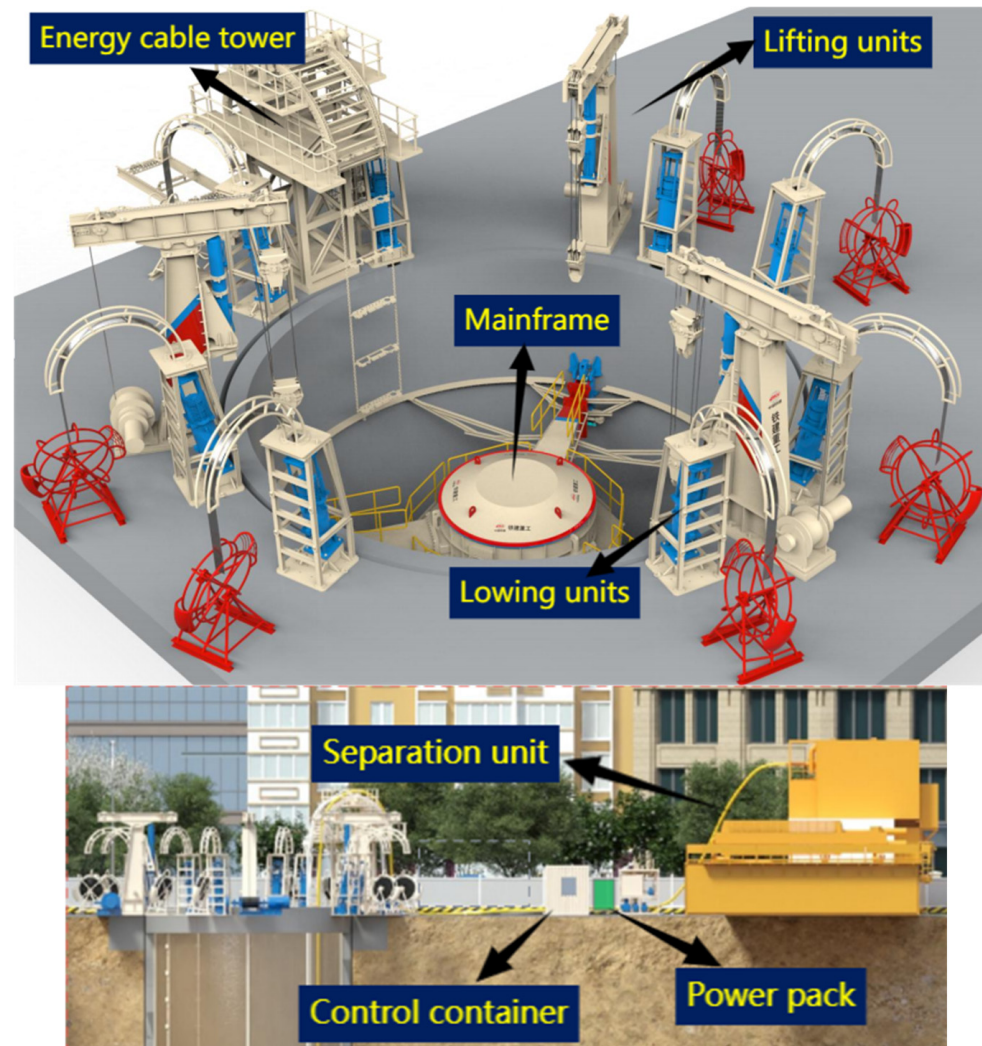


Figure 1. The VSM set-up for the studied project.

- (a) The energy cable tower guides the cables and hoses of the energy chain into the shaft, synchronized with the lowering of the shaft structure;
- (b) The lifting units lift the entire mainframe on steel cables, and the machine position and depth can be adjusted at any time;
- (c) The lowering units lower the entire shaft structure on steel cables attached to the shaft edge;
- (d) The mainframe supports the rotary drive of the telescopic boom and the supply units for the machine;
- (e) The separation unit: the wastewater extracted from the caisson will be directed to the separation unit for treatment and subsequently either partially discharged or recycled;
- (f) The power pack supplies power to the entire VSM for operation;
- (g) The control container: due to the environmental conditions on site, the orientation of the sunken shaft may experience deviations; the control room is equipped to continuously monitor the operational system of the machinery and the orientation of the sunken shaft, enabling immediate adjustments in case of any issues.

The model's lateral boundaries are constrained normally, while the bottom boundary is fixed in place. The displacement controls the sinking of the shaft wall. The load applied to the top ring foundation is determined by subtracting the structure's buoyancy from the total gravitational force of the equipment units, main machine, shaft wall, and bottom ring support beam. This load is then uniformly distributed across the designated load areas. The calculations reveal that the stress on the load area of the lifting unit is 28.3 kPa, while the lowering unit's load area experiences a stress of 552 kPa, with each sinking step contributing an additional 48.7 kPa. The stress on the load area associated with the power winch tower is measured at 178 kPa.

2.4. Structure Design and Parameters of Structures

The subterranean parking garage structure can be roughly categorized into three main components: pile, shaft, and reinforcement structures. The project utilized FLAC^{3D} software to model the overall structure, as depicted in Figure 2. The primary soil layers involved in the project consist of soft soil.

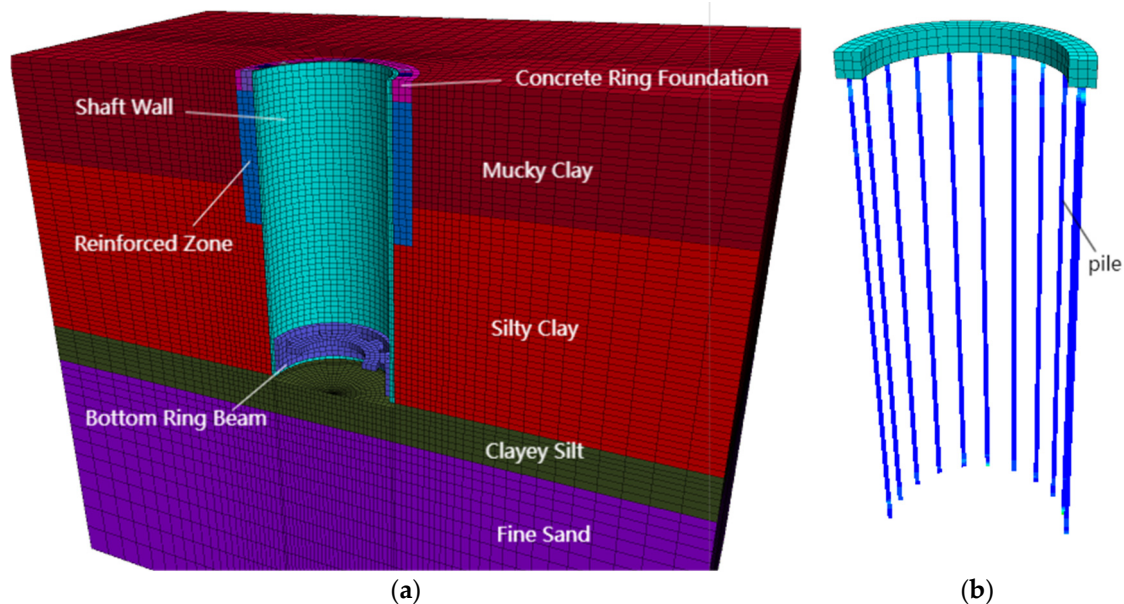


Figure 2. Different views of structure: (a) side view and (b) pile foundation.

The shaft structure comprises a shaft wall and concrete ring foundation. The construction of the shaft wall involves utilizing fragment assembly technology, where factory prefabricated segments are transported to the construction site for assembly. This approach offers enhanced efficiency compared to on-site pouring, stricter quality control due to factory production, reduced on-site noise and pollution during assembly process, and easier disassembly and reuse of prefabricated components.

The pile structure functions as the foundation of the caisson, bearing a significant portion of its load. Active suspension control is executed by jacks while transferring mechanical weight through steel strands to the surface. Consequently, loads are concentrated on the foundation composed of top ring beams and a series of piles.

To mitigate potential deformation during construction, a reinforced structure has been incorporated with a reinforcement zone at depths ranging from 0 to 24 m. Additionally, the bottom ring beam has been designed to prevent excessive horizontal displacement at the bottom of the caisson shaft.

The shaft wall, ring foundation, reinforced zone, and ring support beam are all modeled as solid elements using concrete material, based on an elastic model. For the reinforced zone, the Mohr–Coulomb model is applied. The main model parameters are presented in Table 1.

Table 1. Parameters of structures.

Structure	Shaft Wall	Ring Foundation	Reinforced Zone	Ring Support Beam	Plain Concrete
Bulk modulus, K /[MPa]	1.92×10^4	1.8×10^4	56	1.8×10^4	1.75×10^4
Shear modulus, G /[MPa]	1.44×10^4	1.35×10^4	42	1.35×10^4	1.3×10^4
Cohesion, c /[kPa]	-	-	240	-	-
Friction angle, φ /[°]	-	-	25	-	-
Density, ρ /[kg/m ³]	2500	2500	1900	2500	2350

The piles are modeled using structural elements. The definition of these structural elements must take into account geometrical parameters, material properties, and the coupling spring parameters. Each linear segment between two structural nodes represents a pile element component, and these components are characterized by symmetrical cross-sectional parameters. The stiffness matrix of each pile element is uniform, which not only provides the structural characteristics of a beam but also allows for frictional interaction between the normal and shear directions.

As a result, the pile elements effectively combine the functions of both beams and anchor cables, making them suitable for simulating pile foundations that experience both normal and axial friction forces. This combined functionality allows the model to capture the complex interactions between the pile and surrounding soil, particularly in cases involving uplift forces.

This description integrates the structural element theory into the context of pile modeling, highlighting the dual role of the elements in resisting loads.

The interaction between the piles and the solid elements is realized through coupling springs. These coupling springs are nonlinear and have sliding connectors capable of transmitting forces and moments between the pile nodes and solid elements. The tangential springs work similarly to the tangential action mechanism of grouted anchors, while the normal springs simulate the normal load transmission. They can also simulate the formation of gaps between pile nodes and solid elements, as well as the squeezing effect of the surrounding soil on the pile. A rigid connection is applied between the pile head units and the ring beam, ensuring structural integrity. The main model parameters of the piles are presented in Table 2.

Table 2. Parameters of pile.

Structure	Elastic Modulus E /[MPa]	Poisson's Ratio ν	Cross-Sectional Area A /[L ²]	Outer Length P /[L]	Moment of Inertia (Y-axis) I_y /[L ⁴]	Moment of Inertia (Z-axis) I_z /[L ⁴]	Polar Moment of Inertia J /[L ⁴]	Density ρ /[M/L ³]	Tensile Strength σ_{ty} /[F]
	3×10^4	0.2	1.13	3.77	0.1	0.1	0.2	2400	3.2×10^6
Pile	Normal Stiffness per Unit Length K_n /[F/L ²]			Normal Cohesion per Unit Length c_n /[F/L]			Normal Friction Angle φ_n /[°]		
	2×10^9			2.1×10^5			20		
	Shear Stiffness per Unit Length K_s /[F/L ²]			Shear Cohesion per Unit Length c_s /[F/L]			Shear Friction Angle φ_s /[°]		
	2×10^9			3×10^4			20		

2.5. Constitutive Model and Parameters of Soils

For the soil, the Hardening Soil (HS) model is employed, which is an advanced elastoplastic model capable of capturing the nonlinear and stress-dependent deformation behavior of cohesive soils prior to failure. The HS model distinguishes between loading

and unloading moduli, making it suitable for simulating a wide range of soils, from soft to stiff. The model includes a cap-type yield surface that expands with plastic strain in principal stress space, allowing for the simultaneous consideration of both shear hardening and compression hardening mechanisms. The failure criterion follows the Mohr–Coulomb framework. Additionally, the HS model incorporates stress-dependent parameters which account for the influence of stress paths on soil behavior. Due to its ability to capture complex soil mechanics, the HS model is widely utilized in numerical simulations of deep excavations under various geotechnical conditions and has become one of the most frequently used models in foundation pit engineering. The soil parameters are listed in Table 3.

Table 3. Parameters of soils.

Soils	Mucky Clay	Silty Clay	Clayey Silt	Fine Sand
Reference stress, p^{ref} /[kPa]	100	100	100	100
Poisson's ratio, ν /[MPa]	0.3	0.3	0.3	0.25
Cohesion, c /[kPa]	8	24	11.8	4
Friction angle, φ /[°]	11	21	28	34
Dilatancy angle, Ψ /[°]	0	0	0	4
Secant Young's modulus, E_{50}^{ref} /[MPa]	8.3	22.5	16.8	41.1
Unloading–reloading sec ant Young's modulus, E_{ur}^{ref} /[MPa]	37.8	132	97.5	164.4
Oedometric tangent modulus, E_{oed}^{ref} /[MPa]	18.4	18.9	13.8	41.1
Exponent in power law, m /[-]	0.95	0.9	0.7	0.5
Coefficient of earth pressure for normal consolidation, K_{NC} /[-]	0.81	0.64	0.53	0.44
Failure ratio, R_f /[-]	0.9	0.9	0.9	0.9

2.6. Model Validation

In this study, the sign conventions for soil horizontal displacement (TX) and pile horizontal displacement (CX) are defined as follows: for horizontal displacement, positive values indicate movement toward the center of the shaft, while negative values represent movement away from the shaft. The comparison between the simulated and monitored data primarily focuses on horizontal displacement changes at various depths during different construction stages.

To validate the accuracy of the numerical model, monitoring points were established around the shaft for both the pile (CX1) and the soil (TX1, TX2). As construction progressed, the monitored data were compared with the numerical simulation results, as shown in Figure 3.

During the final sinking stage, the simulated horizontal displacement for both the pile and soil exhibited a trend of increasing and then decreasing with depth. For the pile CX1, the maximum simulated horizontal displacement occurred at a depth of around 40 m, with a value of 12.78 mm, compared to the measured value of 14.51 mm, resulting in a difference of 2 mm. The maximum simulated displacement for the soil TX1 was 12.24 mm, while the measured value was 11.51 mm, with a difference of approximately 1 mm. For the soil TX2, the simulated maximum displacement was 14.78 mm, while the measured value was 9.97 mm, showing a difference of about 5 mm.

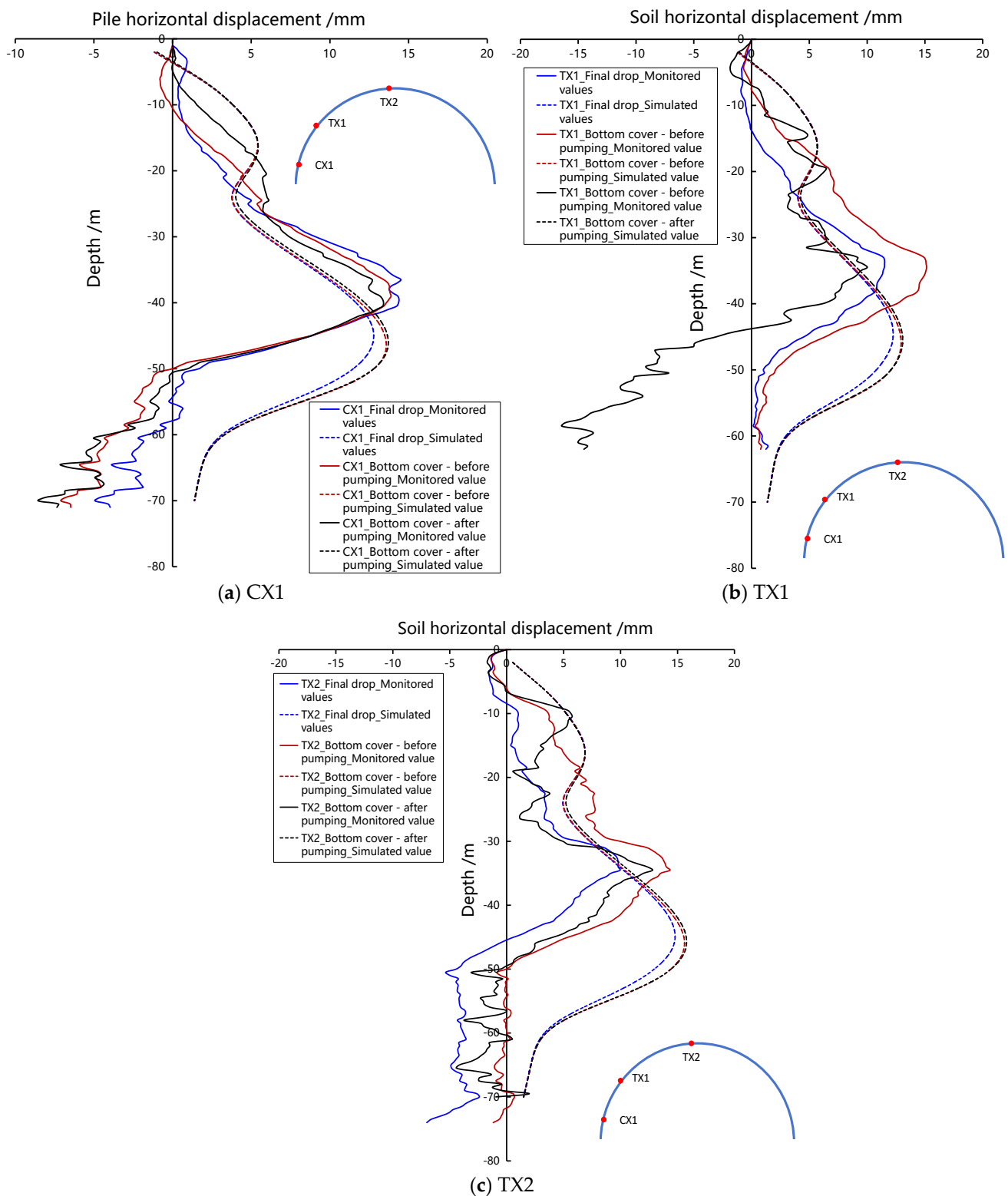


Figure 3. Comparison of simulated and monitored values of horizontal displacement of piles and soils along depth.

In the post-final sinking stages, the horizontal displacement of both the pile and soil continued to follow a consistent pattern with depth. In the stage after sealing and before pumping, the maximum simulated horizontal displacement for the pile CX1 was 13.57 mm, nearly identical to the measured value of 13.88 mm. The differences between the simulated

and measured maximum values for the soil TX1 and TX2 were 2 mm and 1 mm, respectively. After pumping, the simulated and measured values remained aligned, with the difference in the pile CX1 being less than 1 mm, while the differences for the soil TX1 and TX2 were 3 mm each.

Although there were discrepancies between the simulated and monitored data at certain depths, particularly in the post-final sinking stages where outward horizontal displacement was observed, the overall trends closely matched the numerical simulation results. The errors were generally within acceptable limits. Therefore, the model is considered reliable for further numerical analysis.

3. Results: Mechanical Analysis of Pile Foundation

This paper utilizes the pile foundation designed by the project as a base case. The foundation consists of 22 evenly distributed piles under the ring beam, with a spacing of 3.2 m. Each pile is 70 m in length and 1.2 m in diameter. To analyze the behavior of the pile system and soil during excavation, several models were created, keeping all characteristics of the pile unchanged except for one, in order to study the influence of changing characteristics on the pile foundation. The analysis is conducted according to three main stages: “Final drop”, “Bottom cover—before pumping”, and “Bottom cover—after pumping”. These three stages are denoted by the abbreviations “FD”, “PC”, and “PC-d”, respectively. As shown in Figure 4, FLAC^{3D} can simulate the construction phase, presenting the axial force values of the piles in three stages.

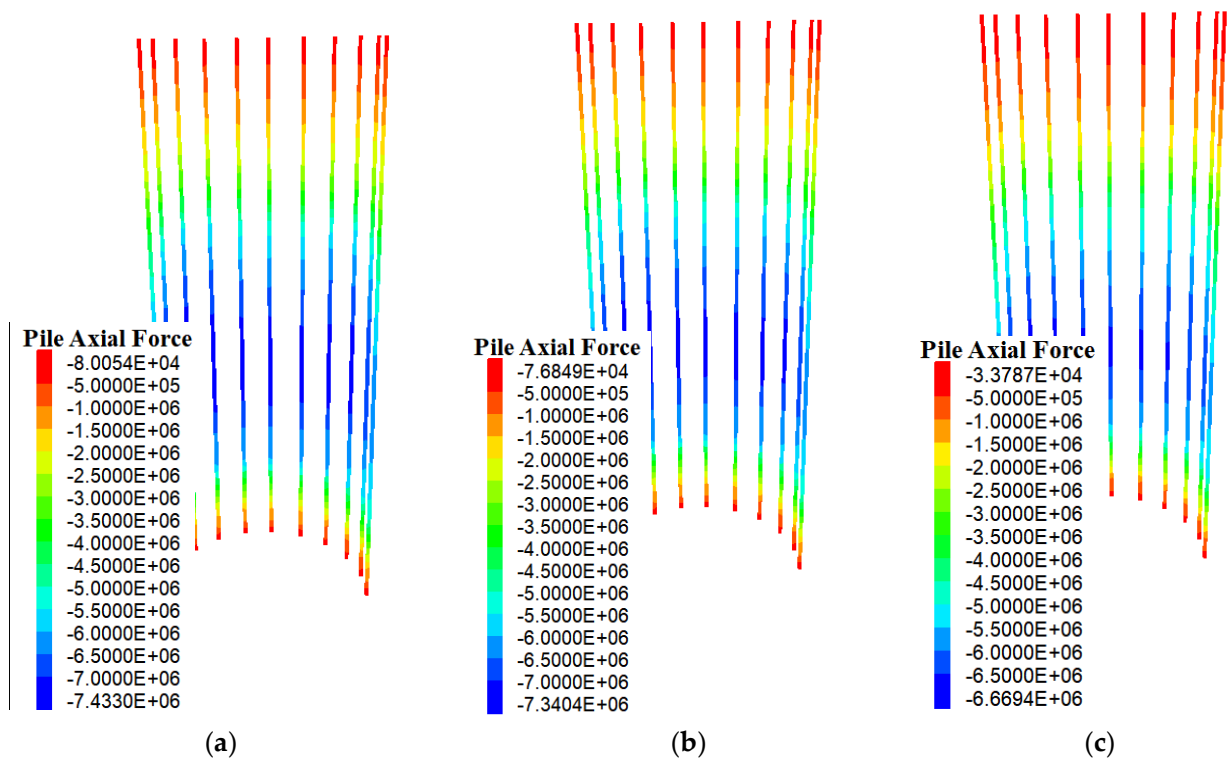


Figure 4. Geometry of piles in three stages using FLAC^{3D} software: (a) “FD” stage (b) “PC” stage and (c) “PC-d” stage.

The division into stages is crucial as the sinking process in caisson foundations exerts significant influence on the structure’s stability. For instance, Jiang et al. (2022) emphasized the importance of monitoring different construction phases to assess structural behavior during underground parking garage construction, and Luo et al. (2022) focused on how the soil and caisson interaction changes during the sinking process in soft-soil environments [20,21]. Similarly, Zhou et al. (2023) studied how deformation mech-

anisms evolve through different stages of caisson installation, underlining the necessity of phase-specific analysis to control deformation effectively in soft soils [22].

In addition to axial force, other parameters can also be obtained through simulation, which is essential for understanding the performance of pile foundations under various conditions.

3.1. Pile Spacing

In the analysis of pile foundations, multiple studies have shown that pile spacing is a critical parameter influencing lateral pile group behavior [23–26]. Rollins et al. (2006) [23,25] conducted extensive load tests and analyses, revealing that pile groups with smaller spacing exhibit significantly different lateral behavior compared to those with larger spacing, especially under seismic loads. Mandolini et al. (2005) [24] emphasized the importance of considering pile spacing in both experimental investigations and design, as it directly impacts the efficiency and performance of pile foundations in various soil conditions. These findings suggest that optimal pile spacing not only improves load distribution but also enhances overall foundation stability.

In order to improve the foundation system and analyze differences in mechanical behavior with varying pile spacing, six different models were established, as outlined in Table 4. These models featured different distances and quantities of piles, with a direct relationship between the number of piles and the resulting pile spacing. It should be noted that parameters such as pile diameter, top ring beam diameter, and soil and concrete properties remained consistent across all models. An analysis was conducted to determine the optimal pile spacing based on parameters such as bending moments, soil deformations, shear stress, and axial forces [27].

Table 4. Number of piles and spacing.

Model	Number of Piles	Spacing (m)
S1	42	1.7
S2	28	2.5
S3	22	3.2
S4	14	5.1
S5	12	5.9
S6	10	7.1

3.1.1. Moment and Internal Force

The maximum and minimum moments of the piles in the z-direction and the displacements of the soil both around the piles and at the excavation face were considered.

The negative bending moment suggests that the pile deflects toward the side of the shaft. Generally, there is an equilibrium between the positive and negative bending moments for each pile spacing scenario in the model. However, as depicted in Figure 5a, during the “FD” stage, when the distance between piles is less than 5.1 m, there is a smaller value of bending moment compared to that of the “bottom cover” stage; this value significantly increases with an increase in pile spacing. When exceeding 5.1 m between piles, the bending moment value of the “FD” stage becomes nearly equivalent to that of the “bottom cover” stage. Additionally, minimal alterations are observed in bending moments during both “PC” and “PC-d” stages, which are also considered highly stressed stages due to maximum system gravity after excavation reaches its highest point and concrete is poured into the shaft. Likewise, an augmentation in pile spacing leads to increased load on each member and a wider span of ring beams between supports, resulting in amplified bending moments for each pile.

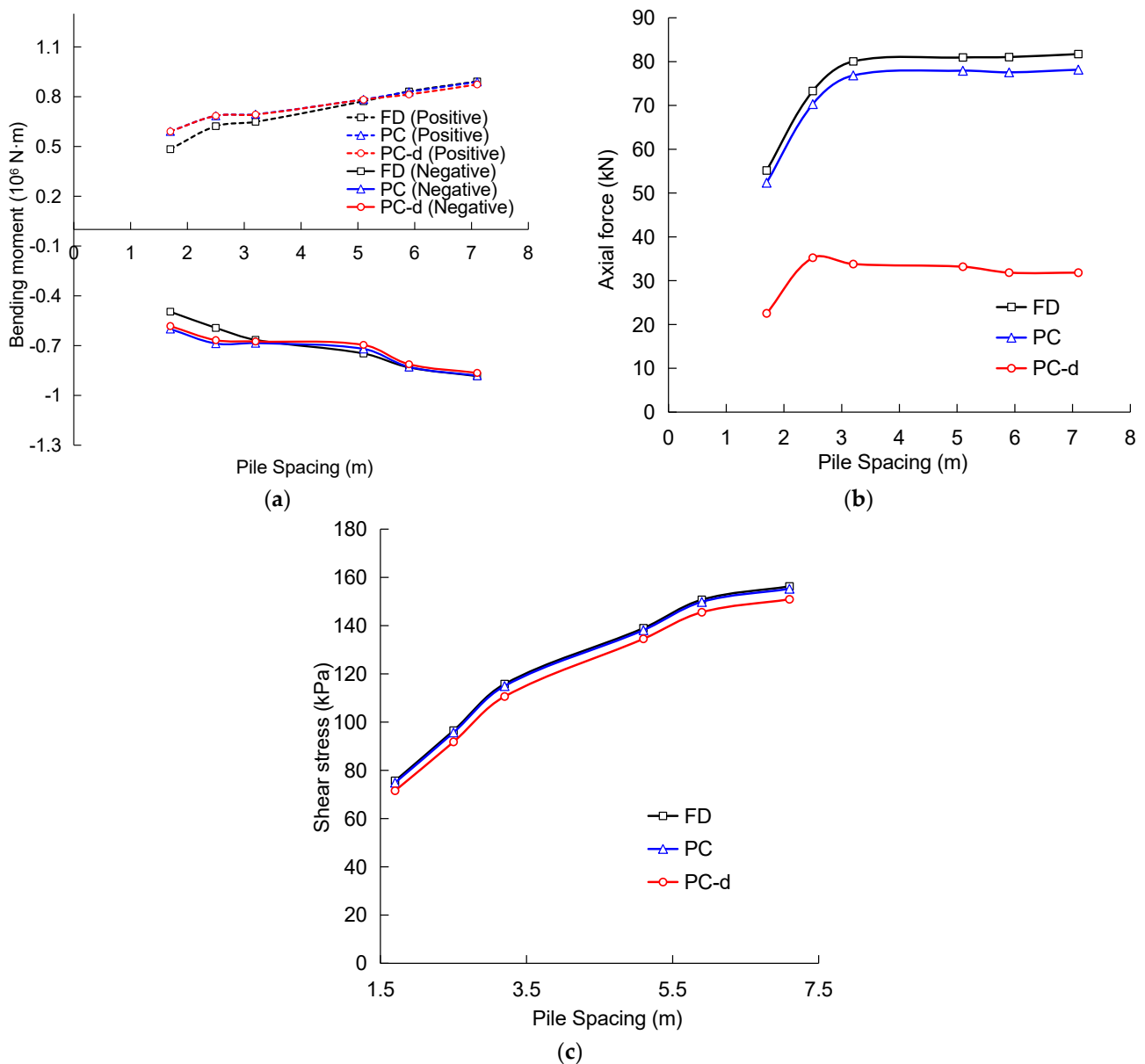


Figure 5. Extreme values of mechanical results of piles for different pile spacing: (a) maximum bending moment about z-axis of pile, (b) maximum axial force in pile, and (c) maximum shear stress in pile.

The axial force, shown in Figure 5b, is significantly influenced by the change in construction stage. Although the “FD” and “PC” stages exhibit similarities, there is a notable reduction in axial force during the “PC-d” stage due to water removal from the shaft, leading to the relaxation of downward pressure on the pile as it experiences buoyancy. The axial force is influenced by the spacing between piles, and it increases as the spacing increases. When the pile spacing reaches 3.2 m, there is a gradual increase in axial force, but the rate of change is relatively small and remains essentially unchanged.

In terms of shear stress, shown in Figure 5c, an increase in the distance between piles results in a decrease in soil density and subsequently reduces its shear resistance. It is noteworthy that the shear resistance of soil is correlated with its density [28]; thus, widening the pile spacing and decreasing the number of piles will make soft soil with lower density more prone to experiencing higher levels of shear stress. Lin et al. (2023) found significant differences in the load-bearing behavior of single piles and pile groups in soils with varying relative densities. As the soil density increases, pile capacity improves significantly [29–33].

3.1.2. Displacement

For displacement, in the absence of a specified coordinate axis direction, positive values represent horizontal movement toward the shaft center. Vertical displacements with positive values indicate upward movement. When the displacement converges toward the interior (or inside the shaft), it is considered positive. Axial forces and stresses are deemed positive if they tend to compress the member at the section being analyzed. Bending moments that deflect the cross-section toward the shaft center are positive. Negative values represent the opposite directions.

To validate the model, several monitoring points were established on site along three distinct directions (L1, L2, and L3) around the shaft's perimeter, as shown in Figure 6a. These points correspond to locations in the numerical model where we collected data. The horizontal displacements of the monitoring piles and soil layers are monitored vertically, as illustrated in Figure 6b. Upon reaching the final excavation depth, the monitored and numerical results are compared. In the L1 and L3 directions, a relatively minor difference can be observed between the numerical values and the measured data, with a maximum deviation of 1.09 mm. In the L2 direction, the maximum difference is 1.76 mm, which is considered acceptable for the purposes of this study.

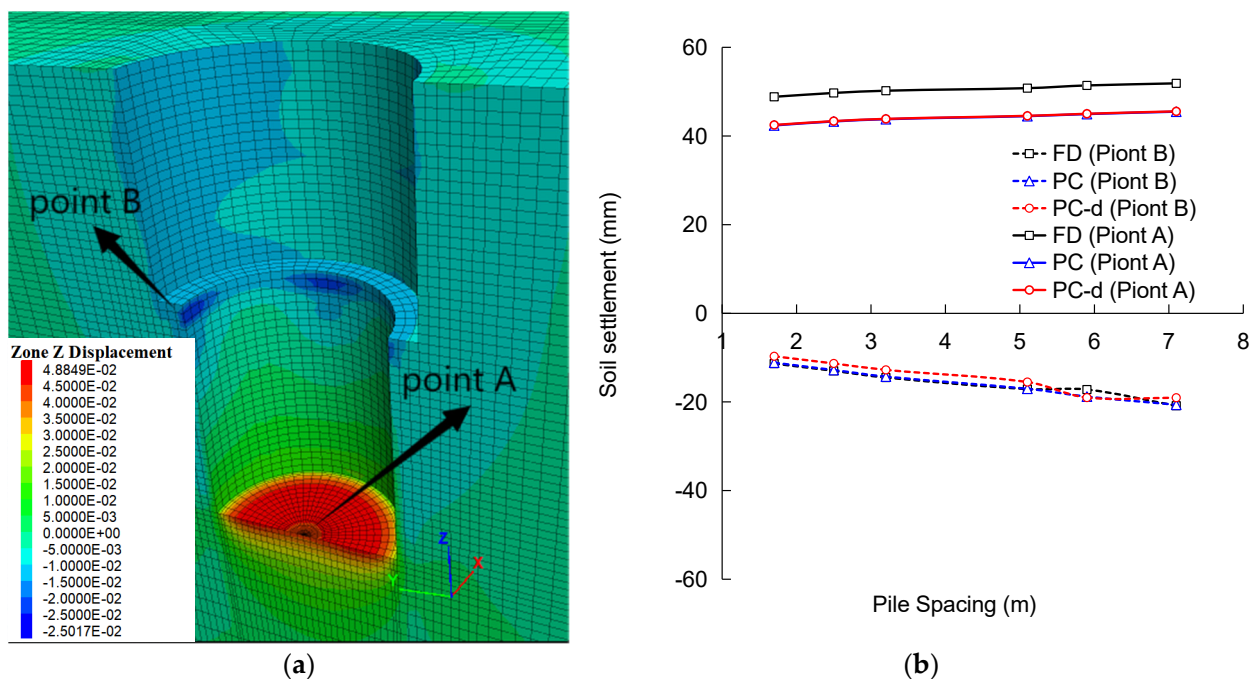


Figure 6. Comparison of numerical values with monitored values: (a) surface settlement; (b) horizontal displacements of piles and soils along depth.

The influence of the caisson leads to the concentration of maximum vertical displacement uplift at “point A”, the center of the soil excavation face at the bottom of the caisson, with the maximum settlement displacement occurring in the soil near the pile, as depicted in Figure 6a below. A specific point named “point B” close to the maximum settlement around the pile is selected for analyzing variations in vertical displacement across different stages.

As depicted in Figure 6b, when the pile spacing varies from 1.7 m to 7.1 m, the pile spacing has minimal impact on the vertical displacement of the soil, and there is a slight increase in vertical displacement with larger pile spacing. The soil settlement around the pile (point B) decreases due to buoyancy effects after pumping, and the vertical displacement remains relatively consistent in other stages. The bottom of the shaft (point A) is primarily influenced by concrete gravity, resulting in similar vertical displacement after the bottom cover, albeit smaller than during the “FD” stage.

3.2. Pile Diameter

The pile diameter is an important parameter that affects the behavior, performance, and design of pile foundations [34–37]. Ashford and Juirnarongrit (2003) [34] highlighted that variations in pile diameter significantly influence the initial modulus of the subgrade reaction, which is essential for understanding the foundation’s response under loading conditions. Comodromos et al. (2009) [35] conducted a comprehensive analysis utilizing experimental data and 3D numerical simulations, emphasizing the necessity of considering pile diameter in both the analysis and design phases to achieve optimal performance.

The selected pile for the Shanghai underground parking garage project is considered the base case. The diameter of the pile is 1.2 m, and any changes in pile diameter will impact material characteristics. During the modeling process, certain material characteristic values will vary with changes in pile diameter [38–40]:

$$S = \frac{\pi}{4} D^2 \quad (1)$$

$$C = \pi D \quad (2)$$

$$moi - y = moi - z = \frac{\pi}{64} D^4 \quad (3)$$

$$moi - polar = moi - y + moi - z = \frac{\pi}{32} D^4 \quad (4)$$

where D represents the unit of pile diameter in meters, C represents the unit of pile circumference in meters, S represents the unit of pile cross-sectional area in square meters, $moi-y$ represents the unit of the Y-axis moment of inertia in cubic meters to the fourth power, $moi-z$ represents the unit of the Z-axis moment of inertia in cubic meters to the fourth power, and $moi-polar$ represents the unit of the polar coordinate moment of inertia in cubic meters to the fourth power.

The base case diameter of 1.2 m is subject to reduction or enlargement by factors of 0.5, 0.75, 1.15, 1.25, and 1.5. And based on these formulas, the moments of inertia (Y, Z, and polar) as well as the cross-section and perimeter of each pile can be calculated, as presented in Table 5.

Table 5. Models with different pile diameters.

Model	D (m)	C (m)	S (m ²)	$moi-y$ (m ⁴)	$moi-z$ (m ⁴)	$moi-polar$ (m ⁴)
D1	0.6	1.89	0.28	0.006	0.006	0.013
D2	0.9	2.83	0.64	0.032	0.032	0.064
D3 (base case)	1.2	3.77	1.13	0.1	0.1	0.2
D4	1.4	4.41	1.54	0.189	0.189	0.378
D5	1.5	4.72	1.77	0.249	0.249	0.498
D6	1.8	5.67	2.55	0.516	0.516	1.033

These material property values are utilized for generating models of various pile diameters in the software FLAC^{3D}, aiming to facilitate the investigation of the impacts of different pile diameters on the soil and structure.

3.2.1. Moment

This study observed a balance between the maximum and minimum torques within the specified range. Furthermore, there is a notable increase in torques with an increase in pile diameter. However, between 1.4 m (D4) and 1.5 m (D5) diameters, piles exhibit similar behaviors in response to flexural moments generated by VSM loads, as shown in Figure 7. In all three stages, the maximum negative bending moment is smaller when the pile diameter ranges from 1.4 m to 1.8 m. Additionally, during the “FD” stage, with a pile

diameter ranging from 1.2 m to 1.8 m, the maximum positive bending moment is also smaller compared to other stages.

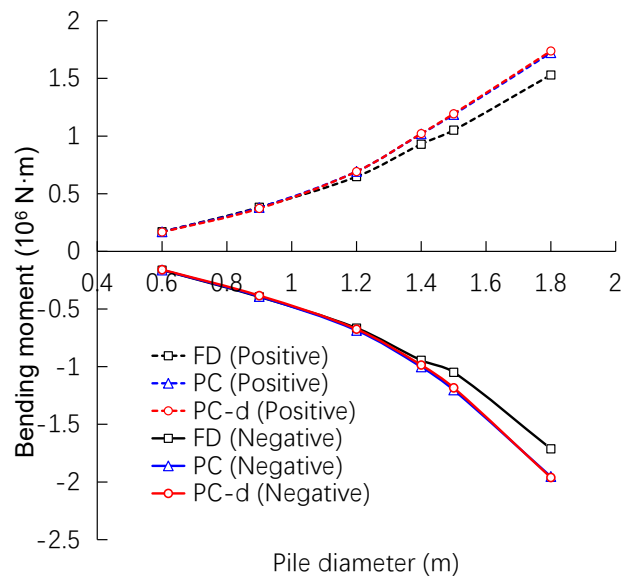


Figure 7. The maximum bending moments along the z-axis of the piles for different pile diameters.

3.2.2. Displacement

The vertical displacement of the excavation face and around the pile varies with changes in pile diameter. Given the importance of accurately reflecting the trend in pile diameter, point C is designated as the circumference point with significant vertical displacement around pile 1, situated at a depth of approximately 27 m, as depicted in Figure 8a. Also, the central point of the excavation face remains designated as point A.

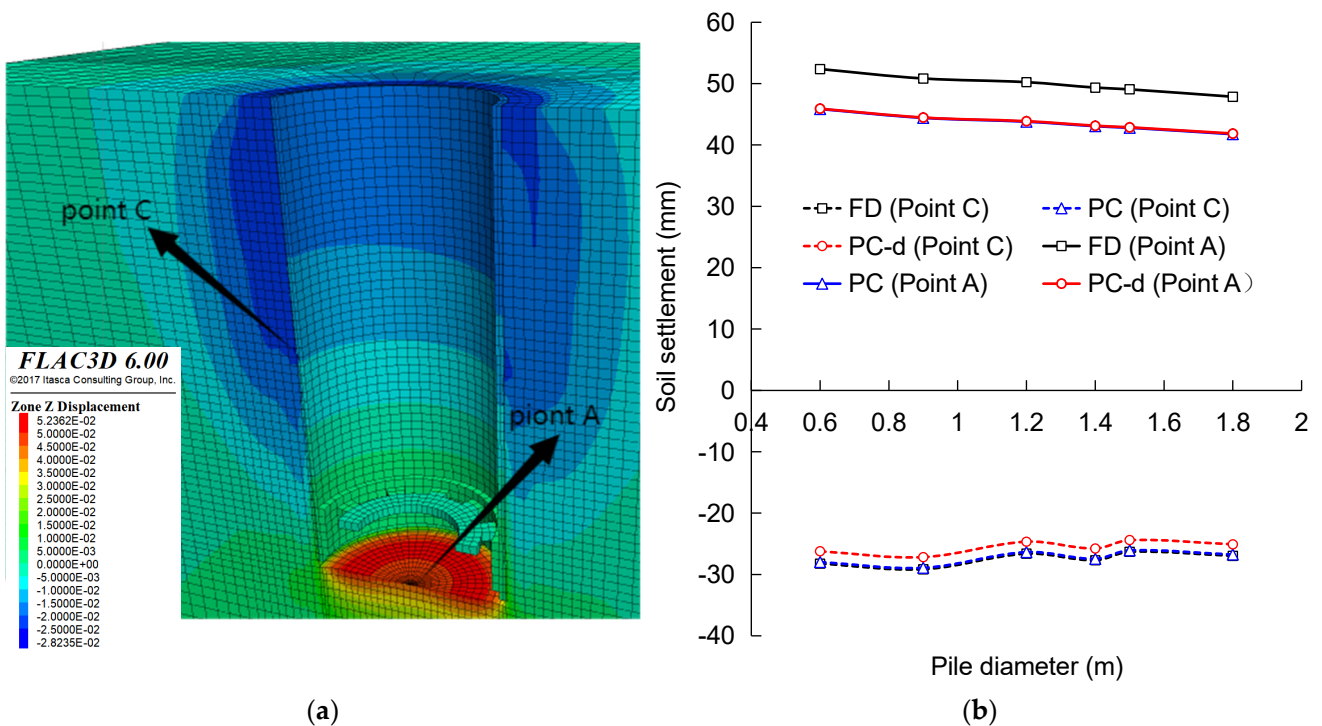


Figure 8. Points A and C's (a) location and (b) displacement for different pile diameters.

As the diameter of the piles increases, as shown in Figure 8b, there is a decreasing trend in soil deformation in both the lower part of the excavation area and its surrounding region. In essence, smaller diameters result in greater soil deformation, while larger diameters lead to reduced displacement. It can be observed that alterations in cross-sectional size have a more pronounced impact on deformation around the excavation than at its base due to the role of piles not only in supporting VSM loads but also in contributing significantly to excavator sidewall stability.

Similarly, it was observed that during the “FD” stage, there was substantial deformation of the excavation face which sharply decreased when bottom capping occurred and water was pumped from the shaft. Furthermore, deformation around the excavation surface primarily depends on foundation performance; therefore, no discernible differences were noted among the “FD”, “PC”, and “PC-d” stages.

3.2.3. Axial and Shear Stress

The variation in pile diameter has a significant impact on shear stress [41]. As depicted in Figure 9a, it is evident that as the circumference and cross-sectional area of the pile increase, the shear stress in the soil decreases. This is because with a larger diameter, the load distribution on the ground becomes more uniform, leading to the increased bearing capacity of the material. Similarly, increasing the diameter densifies the material, thereby improving the soil’s shear stress resistance. Regardless of which excavation stage it is in, due to effective reinforcement and anti-floating measures, there is not much change in stress state for models with similar pile diameters during different construction stages.

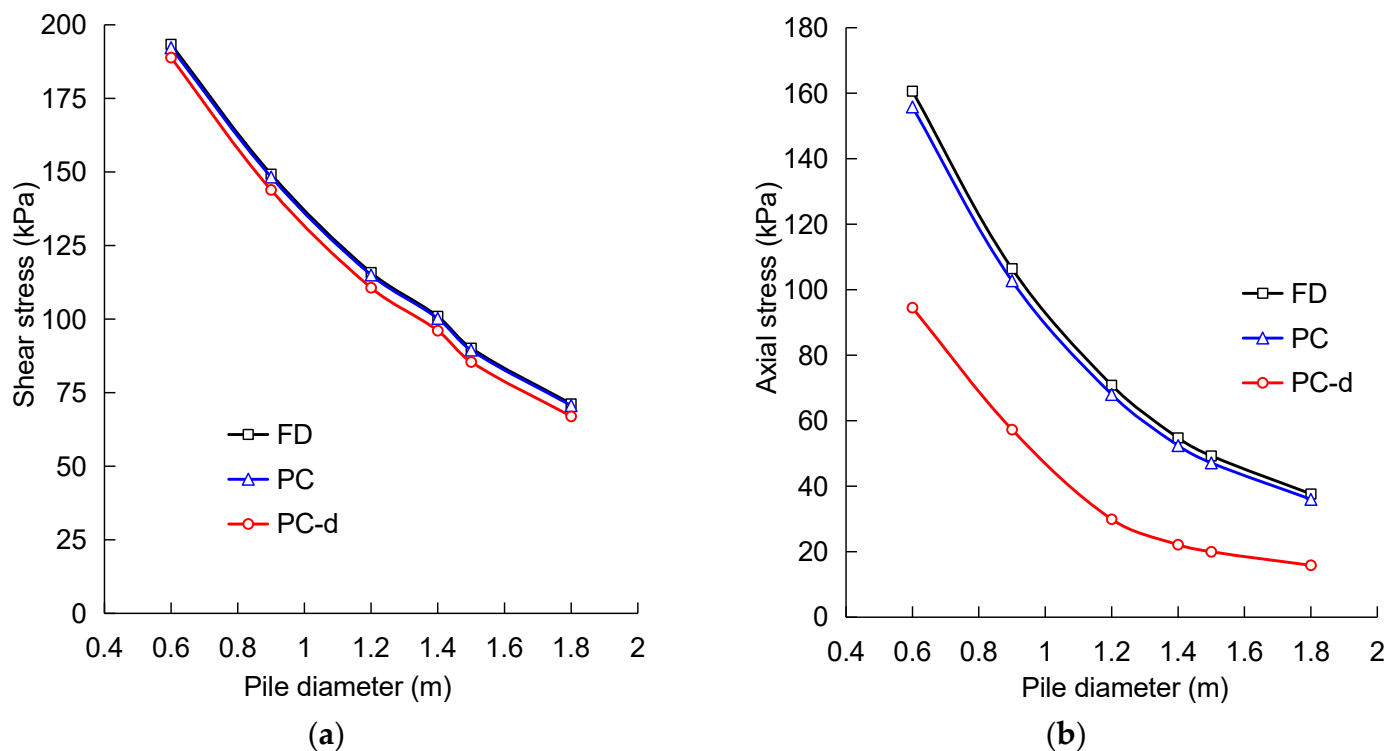


Figure 9. Extreme values of mechanical results of piles for different pile diameters: (a) maximum shear stress and (b) maximum axial stress in pile.

In terms of axial stress, as the diameter of the pile increases, the axial stress tends to decrease significantly. However, the axial stress is affected by the excavation stage and the change in the cross-sectional size of the pile. The curve representing axial stress levels flattens when the pile diameter reaches 1.2 m. As depicted in Figure 9b, it is evident that load distribution improves with increasing diameter. The axial stress decreases after the shaft is drained, and the axial stress during the “FD” stage and “PC” stage is almost the

same. This is because after the excavation is completed, the caisson is in a saturated state, and the stress hardly changes. Pender et al. (2007) found that larger pile diameters increase pile head lateral stiffness and improve overall foundation stability. Larger diameters help dissipate stress more effectively under lateral loads [41].

3.3. Pile Length

The length of the pile is a critical factor in the VSM method and has a significant impact on the overall economic cost [42–44]; the length of the pile plays a pivotal role in optimizing the performance of pile groups and piled raft systems. Leung et al. (2010) [42] demonstrate through theoretical analysis that the optimization of pile length can significantly enhance load distribution and reduce settlement in pile foundations. This is echoed by Randolph (2003) [43] who emphasizes the interplay between scientific principles and empirical evidence in the design of pile foundations, underscoring that insufficient pile length can lead to inadequate load-bearing capacity and potential structural failures. Moreover, Akl et al. (2014) [44] investigate how variations in pile configurations and lengths impact the behavior of pile raft foundations, highlighting that the appropriate selection of pile length not only improves the foundation's overall performance but also influences the structural integrity of the superstructure. Therefore, a comprehensive understanding of pile length optimization is essential for the effective design of pile foundations, ensuring safety and sustainability in geotechnical engineering practices.

Selecting an appropriate pile length requires conducting mechanical analyses on established models for piles of different lengths. As part of this process, as shown in Table 6, 11 caisson models are simulated, each composed of piles with varying lengths from 24 m to 75 m.

Table 6. Models with different pile lengths.

Model	L1	L2	L3	L4	L5	L6	L7	L8	L9	L10	L11
Length (m)	24 m	30 m	35 m	40 m	45 m	50 m	55 m	60 m	65 m	70 m	75 m

3.3.1. Moment

In the studied range, as shown in Figure 10, balance between the maximum and minimum torques is observed. As the pile length increases, the positive bending moment fluctuates continuously within the range from 600 kN·m to 810 kN·m, while the negative bending moment similarly fluctuates within the range from −600 kN·m to −810 kN·m. Overall, the bending moment gradually decreases with increasing pile length. The maximum value of bending moment occurs at a pile length of 24 m. At a pile length of 30 m, both positive and negative bending moments decrease abruptly. When the pile length reaches 35 m, there is partial recovery in both positive and negative bending moments before they slowly decrease again.

3.3.2. Displacement

By studying the curve trends and vertical displacement behavior associated with the excavation phase, as shown in Figure 11, it can be observed that during the “FD” stage, there is a larger magnitude of vertical displacement compared to other stages. This is attributed to a sharp reduction in deformation of the excavation face after bottom sealing and pumping from the shaft. Additionally, deformations around the excavation face are primarily influenced by the foundation, hence exhibiting consistent behavior across the “FD”, “PC”, and “PC-d” stages without significant differences. The settlement influence around the pile manifests as an upward bulge. With increasing pile length, there is a slight increase in the maximum vertical displacement around the pile from 24 m to 30 m. Subsequently, from a pile length of 30 m to 65 m, the maximum vertical displacement around the pile continues to decrease and remains relatively constant between 65 m and 70 m. After reaching 75 m, the vertical displacement gradually decreases again. Overall, as

the pile length increases, the maximum vertical displacement around the pile decreases; in other words, with greater pile length, there is less uplift of soil mass around the pile. As the pile length increases, soil deformation in the lower and surrounding areas of the excavation zone shows a decreasing trend. Smaller pile lengths result in greater soil deformation, while larger pile lengths lead to smaller displacement amounts.

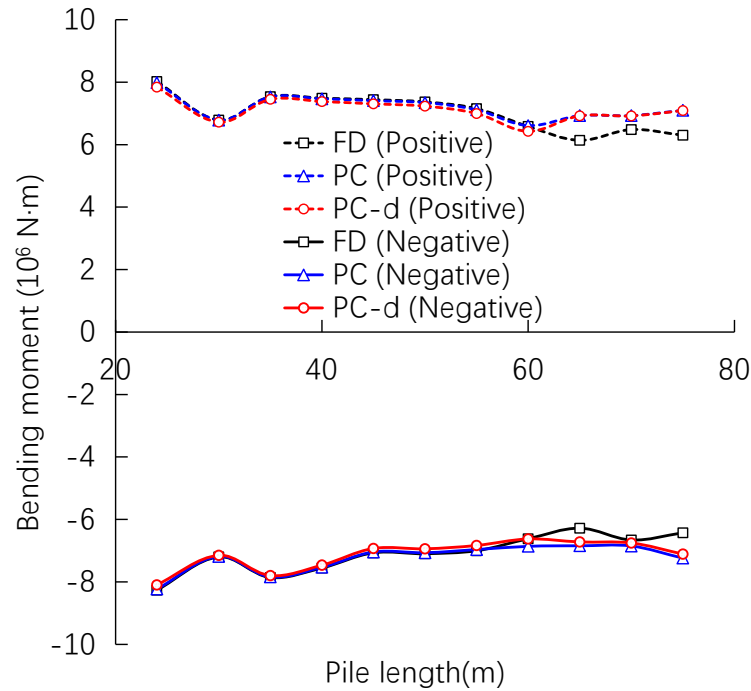


Figure 10. The maximum bending moments along the z-axis of the piles for different pile lengths.

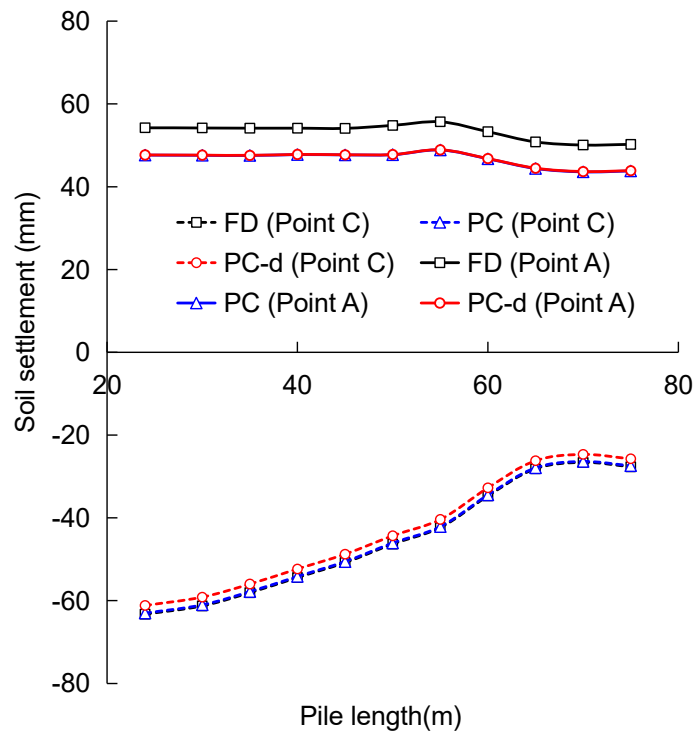


Figure 11. Soil vertical displacement around the pile for different pile lengths.

Unlike other pile parameters, the pile length has a significant impact on soil settlement around the pile. The change in pile length has a greater effect on vertical displacement

around the pile than on vertical displacement at the excavation face. This is because piles not only bear the load generated by vertical stress increases due to construction activities but also play an important role in stabilizing the sidewalls of excavations. Their variations have a greater influence on deformations around excavations than those at the bottom of shafts. When the pile length is sufficiently long, its support effect on excavation sidewalls reaches saturation, and subsequent settlement around the pile is no longer affected by changes in pile length.

3.3.3. Axial and Shear Stress

As the pile length increases, as shown in Figure 12a, the axial stress also increases. Before reaching a length of 30 m, the stress behavior of shorter piles differs significantly from that of longer ones. The construction phase has minimal impact on this behavior. After 30 m, the axial stress during the “PC-d” stage is notably lower than in other stages due to reduced self-weight after pumping, leading to decreased axial stress.

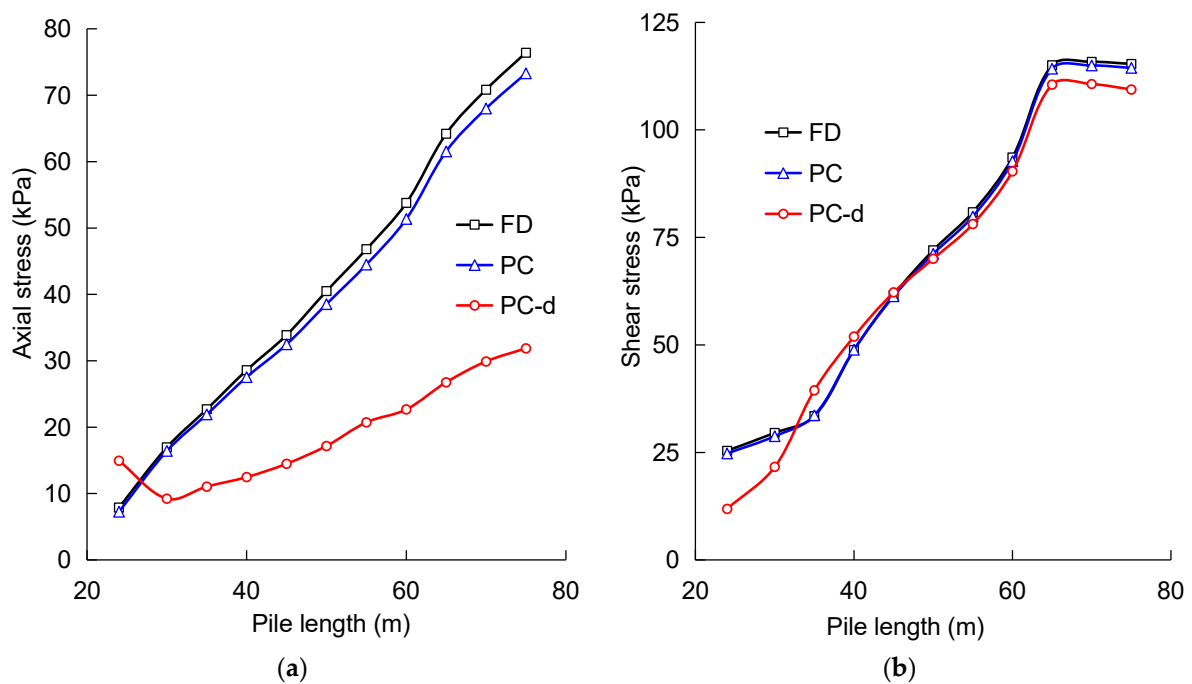


Figure 12. Extreme values of mechanical results of piles for different pile lengths: (a) maximum axial stress and (b) maximum shear stress in pile.

Shear stress increases with pile length and remains relatively consistent across different stages after 30 m; in other words, the construction phase has minimal influence on shear stress. Additionally, as the shaft depth is only about 51 m, when the pile length exceeds 65 m, it surpasses the range of influence on shear stress from the shaft depth. At this point, shear stress reaches saturation, and even though the pile length continues to increase beyond this point, under conditions where the shaft depth is less than the pile length, the received shear stress remains nearly constant. Therefore, as shown in Figure 12b, shear stress remains unchanged after reaching a length of 65 m.

4. Discussion

4.1. Pile Spacing and Diameter Design

When designing pile parameters, it is crucial to consider not only the individual impact of each parameter on the pile but also the interactions among different parameters [45,46]. This study has investigated the effects of pile spacing, diameter, and length on the mechanical properties of both the soil and structure. Pile spacing is usually required to be more than

twice the pile diameter to ensure sufficient load distribution and avoid pile interference, which is widely accepted in geotechnical engineering practice.

Research shows that pile spacing and diameter play pivotal roles in optimizing foundation performance. For instance, Rollins et al. (2006) [23] and Garala and Madabhushi (2021) [27] confirmed that pile interactions can reduce load-bearing capacity when the spacing is too small, which mirrors the findings in this study regarding potential interference between piles. Moreover, Pender et al. (2007) [37] and Sun et al. (2022) [36] demonstrated that larger pile diameters improve lateral stiffness and stability, yet cost increases significantly as the diameter increases. Thus, a balance between pile diameter, pile spacing, and cost-efficiency must be considered. Gavin and O’Kelly (2007) [33] also noted that improper pile spacing could lead to increased soil settlement, reinforcing the need for adequate spacing in the different models.

When the spacing between piles is appropriate, the pile foundation can better distribute the load, making the entire foundation system more stable. This helps avoid soil settlement and uneven settlement due to concentrated loads. If the spacing between piles is too small, they may interfere with each other, leading to negative effects. For example, the construction of one pile may adversely affect the load of adjacent piles, or the soil between adjacent piles may affect both piles, reducing the bearing capacity of the entire pile foundation. The gap between piles allows the soil to effectively transmit the load. This helps ensure that the load is evenly distributed among the piles and reduces soil stress concentration. If the spacing between piles is too small, soil settlement may occur in the gap between piles, affecting the stability of the entire pile group. Appropriate spacing help reduce this effect. Appropriate pile spacing also helps with construction operations, providing enough space for drilling, pouring concrete, etc. This can avoid affecting the structural stability and bearing capacity of the entire foundation system due to limited construction operations.

It has been shown through previous studies that the larger the diameter of the pile, the better the soil and mechanical properties, and the D6 model performs best in underground parking garage projects. However, the performance is better when the spacing between piles is moderate. In the previous analysis, the car park project performed better with a spacing of 3.2 m (S3 model). However, the minimum spacing requirement for the D6 model is 3.6 m, and the spacing of 3.2 m for the S3 model does not meet the requirements. The use of other pile diameters should be considered. It is worth noting that the increase in pile diameter will result in an increase in cost, while the increase in spacing between piles and the reduction in the number of piles will result in a decrease in cost. Therefore, in the selection of pile diameter, spacing between piles, and the number of piles, cost is also an important factor affecting design, especially for larger pile diameters, such as 1.5 m (D5) or 1.4 m (D4), as soil displacement will be reduced, but it is important that the cost will increase significantly. Therefore, the D3 model with a pile diameter of 1.2 m has more advantages than other models because its deformation is acceptable and controllable, and the spacing between piles is also large enough, which is why the underground parking project ultimately included a pile diameter of 1.2 m.

4.2. Pile Length Design

When the pile length is too short, there is significant settlement of the soil around the pile in the model, indicating that inadequate pile length leads to insufficient support for the foundation. For example, in underground parking garage project, models L1 to L3 performed poorly in all aspects and did not meet the basic requirements of the project. Models L4 to L11 demonstrated improved performance as pile length increased, effectively preventing excessive deformation of the excavation surface and surrounding soil. When reaching a length of 65 m (models L9 to L11), the models exhibited stable and good performance in preventing soil deformation. With increasing length, axial loads continued to increase, and axial stress also increased continuously. In summary, pile lengths should not be too short because inadequate lengths cannot provide sufficient

support for the surrounding soil. Pile lengths should also not be excessively long; previous studies have shown that after reaching a certain length, the support capacity will plateau. Further increases in length will only lead to continuous increases in axial stress, with negative effects.

4.3. Comparing Vertical Shaft Sinking Machine (VSM) with Other Methods

This study compares the performance of Vertical Shaft Sinking Machine (VSM) technology with traditional methods like pneumatic caissons and the Super Open Caisson System (SOCS). The VSM offers significant advantages due to its automated control, enabling real-time adjustments and minimizing the risks associated with soil movement. In contrast, pneumatic caissons and the SOCS rely on manual or phased processes, which slow down excavation and increase complexity. The VSM achieves excavation rates of up to 4 m per day, significantly shortening project timelines, and is adaptable to a wide range of geological conditions, including soft soils, soft rock, and high-water-pressure environments. However, its higher initial cost, due to specialized equipment, makes it less suitable for smaller projects.

A comparative analysis of these methods is summarized in Table 7.

Table 7. Comparative analysis of shaft sinking methods.

Criterion	VSM Technology	Pneumatic Caisson	SOCS
Precision and Control	High automation, real-time monitoring	Limited control with air pressure	Manual intervention and stabilization needed
Excavation Speed	Up to 4 m/day	Slower due to manual processes	Moderate, multi-phase excavation
Geological Adaptability	Effective in soft soil and soft rock, and under high water pressure	Less effective in high-water-pressure conditions	Requires additional stabilization measures
Environmental Impact	Low noise and vibration, suitable for urban areas	Higher noise and disruption	Moderate impact, phased processes
Initial Cost	High due to specialized equipment	Lower, more cost-effective for small projects	Higher due to complexity

In terms of pile foundation design, the VSM method introduces unique load-bearing considerations compared to the other sinking methods. In these methods, the shaft wall primarily sinks under its own weight, and the piles support lateral loads. However, with the VSM, the load is transmitted through suspension systems to the ring beams and then to the piles, meaning the vertical load on the piles must also be accounted for. Vertical loads induce axial compression, enhancing the pile's resistance to overturning and bending, while also increasing deformation and settlement at the pile base. This necessitates greater emphasis on pile stiffness to balance vertical and lateral loads and control bending deformation.

Furthermore, since this project is located in a soft-soil region, diaphragm walls were introduced to enhance soil stability. The combination of shallow diaphragm walls and deep pile foundations forms a composite support system, increasing overall lateral stiffness and reducing horizontal displacement and settlement. However, while diaphragm walls improve stability, they also add complexity and cost to the construction process, especially in soft-soil or deep excavation areas. Numerical analysis is essential to optimize both economic efficiency and structural stability. The VSM, with its precision, efficiency, and lower environmental impact, represents a promising direction for future urban underground construction, particularly in complex geotechnical environments where minimizing disruption is crucial.

5. Conclusions

This study, focused on the underground parking garage project in Jing'an District, Shanghai, investigates the role of pile foundations in the Vertical Shaft Sinking Machine (VSM) method under soft-soil conditions. Using FLAC^{3D} simulations, it offers significant insights for both research and practical engineering applications.

The findings underscore three key parameters: pile diameter, spacing, and length.

1. **Pile Diameter:** A pile diameter of 1.2 m strikes a balance between load-bearing performance and construction costs, effectively reducing soil settlement and shear deformations. While increasing the diameter enhances capacity and minimizes deformation, it also raises costs, so balancing performance with economic feasibility is crucial.
2. **Pile Spacing:** spacing that is too narrow leads to stress concentration, while overly wide spacing causes soil relaxation, both of which can compromise structural stability.
3. **Pile Length:** Optimizing pile length is critical for controlling settlement. Insufficient length leads to deformation, while excessively long piles result in diminishing returns without added benefits, making careful optimization necessary to ensure both structural effectiveness and cost-efficiency.

This study also highlights the interplay between these parameters, indicating that adjustments in spacing may be needed as the pile diameter increases to ensure overall stability. Maintaining spacing of at least twice the pile diameter is essential for uniform load distribution and foundation stability.

In conclusion, this study offers practical recommendations for optimizing pile foundation design in VSM applications, especially in soft-soil environments. While specific to Shanghai's geology, the findings can inform further studies across different regions.

Author Contributions: T.L.: conceptualization, methodology, and writing—original draft; Z.L. and C.M.: investigation and writing—review and editing; Z.X., L.Y. and X.Z.: validation, supervision, and writing—review and editing; K.L.: conceptualization and methodology. All authors have read and agreed to the published version of the manuscript.

Funding: This research was funded by the Science and Technology Project of Guangzhou Municipal Construction Group Co., Ltd. (BH20230317604) and the Research Project of the Department of Housing and Urban Rural Development of Guangdong Province (2023-K9-240562).

Data Availability Statement: Some or all of the data, models, or code that support the findings of this study are available from the corresponding author upon reasonable request.

Conflicts of Interest: The authors declare no conflict of interest. This study received funding from the Science and Technology Project of Guangzhou Municipal Construction Group Co., Ltd. The funder was not involved in the study design, collection, analysis, interpretation of data, the writing of this article or the decision to submit it for publication.

References

1. Luo, M.; Lau, N. Increasing Heat Stress in Urban Areas of Eastern China: Acceleration by Urbanization. *Geophys. Res. Lett.* **2018**, *45*, 13–60. [[CrossRef](#)]
2. Valenzuela-Levi, N. Why Do More Unequal Countries Spend More on Private Vehicles? Evidence and Implications for the Future of Cities. *Sustain. Cities Soc.* **2018**, *43*, 384–394. [[CrossRef](#)]
3. Li, J.; Walker, J.L.; Srinivasan, S.; Anderson, W.P. Modeling Private Car Ownership in China: Investigation of Urban Form Impact across Megacities. *Transp. Res. Rec.* **2010**, *2193*, 76–84. [[CrossRef](#)]
4. Broere, W. Urban Problems—Underground Solutions. In Proceedings of the 13th World Conference of ACUUS: Underground Space Development—Opportunities and Challenges, Singapore, 7–9 November 2012; pp. 1–12.
5. Ushakova, A. Development of Underground Space as Transportation Problem Solution in St. Petersburg. *Procedia Eng.* **2016**, *165*, 166–174. [[CrossRef](#)]
6. Cui, Z.-D.; Zhang, Z.-L.; Yuan, L.; Zhan, Z.-X.; Zhang, W.-K. *Design of Underground Structures*; Springer: Singapore, 2020; ISBN 9811377324.
7. Goel, R.K.; Singh, B.; Zhao, J. *Underground Infrastructures: Planning, Design, and Construction*; Butterworth-Heinemann: Oxford, UK, 2012; ISBN 0123977673.

8. Leung, C.F.; Shen, R.F. Performance of Gravity Caisson on Sand Compaction Piles. *Can. Geotech. J.* **2008**, *45*, 393–407. [[CrossRef](#)]
9. Leung, C.F.; Lee, F.H.; Khoo, E. Behavior of Gravity Caisson on Sand. *J. Geotech. Geoenviron. Eng.* **1997**, *123*, 187–196. [[CrossRef](#)]
10. Tong, B.; Schaefer, V.R. Optimization of Vibrocompaction Design for Liquefaction Mitigation of Gravity Caisson Quay Walls. *Int. J. Geomech.* **2016**, *16*, 04016005. [[CrossRef](#)]
11. Frey, S.; Schmaeh, P. The Role of Mechanized Shaft Sinking in International Tunnelling Projects. In *Tunnels and Underground Cities. Engineering and Innovation Meet Archaeology, Architecture and Art*; CRC Press: Boca Raton, FL, USA, 2019; pp. 2119–2128.
12. Kodaki, K.; Nakano, M.; Maeda, S. Development of the Automatic System for Pneumatic Caisson. *Autom. Constr.* **1997**, *6*, 241–255. [[CrossRef](#)]
13. Tanimura, D.; Ueda, J.; Tani, Y. Large-Scale Vertical Shaft Excavation Using Super-Open Caisson System. Construction of Tamasato Vertical Shaft (Ishioka Vertical Shaft No. 5); Jidoka Open Caisson Koho Ni Yoru Daikibo Tatekui No Kussaku. Tamasato Tateko (Ishioka Dai5 Tateko) Shinsetsu Koji. *Kensetsu No Kikaika* **1998**, *581*, 9–14.
14. Neye, E.; Burger, W.; Rennkamp, P. Rapid Shaft Sinking. *Min. Rep.* **2013**, *149*, 250–255. [[CrossRef](#)]
15. Schmäh, P. Vertical Shaft Machines. State of the Art and Vision. *Acta Montan. Slovaca* **2007**, *12*, 208–216.
16. Ranzinger, M.; Hudej, M. Vertical Shaft Sinking for Underground Transportation Purposes in Slovenia. In Proceedings of the Vertical and Decline Shaft Sinking: Good Practices in Technique and Technology, International Mining Forum 2015, Sydney, Australia, 4–6 November 2015; CRC Press: Boca Raton, FL, USA, 2015; p. 65.
17. Sun, Y.; Li, Z. Analysis of Deep Foundation Pit Pile-Anchor Supporting System Based on FLAC3D. *Geofluids* **2022**, *2022*, 1699292. [[CrossRef](#)]
18. Prakash, S.; Sharma, H.D. *Pile Foundations in Engineering Practice*; John Wiley & Sons: Hoboken, NJ, USA, 1991; ISBN 0471616532.
19. Lei, M.; Luo, S.; Chang, J.; Zhang, R.; Kuang, X.; Jiang, J. Fluid–Solid Coupling Numerical Analysis of Pore Water Pressure and Settlement in Vacuum-Preloaded Soft Foundation Based on FLAC3D. *Sustainability* **2023**, *15*, 7841. [[CrossRef](#)]
20. Jiang, H.; Bao, H.; Lin, Y. Research and Application of Design and Construction Technology of Assembled Shaft: A Case Study of a Sinking Shaft Underground Parking Garage in Nanjing, China. *Tunn. Constr.* **2022**, *42*, 463–470.
21. Luo, W.; Lin, H.; Huang, W.; Zhao, X.; Chen, Y.; Wang, S.; Li, T.; Zhang, L.; Liu, J.; Zhou, M. Undrained Sinking Caisson Construction Technology of a 28.4 m Deep Shaft in Soft Soils. *Spec. Struct.* **2022**, *39*, 113–119.
22. Zhou, J.; Liu, C.; Xu, J.; Zhang, Z.; Li, Z. Deformation Mechanism and Control of In-Situ Assembling Caisson Technology in Soft Soil Area under Field Measurement and Numerical Simulation. *Materials* **2023**, *16*, 1125. [[CrossRef](#)]
23. Rollins, K.M.; Olsen, K.G.; Jensen, D.H.; Garrett, B.H.; Olsen, R.J.; Egbert, J.J. Pile Spacing Effects on Lateral Pile Group Behavior: Analysis. *J. Geotech. Geoenviron. Eng.* **2006**, *132*, 1272–1283. [[CrossRef](#)]
24. Mandolini, A.; Russo, G.; Viggiani, C. Pile Foundations: Experimental Investigations, Analysis and Design. In Proceedings of the 16th International Conference on Soil Mechanics and Geotechnical Engineering; IOS Press: Amsterdam, The Netherlands, 2005; pp. 177–213.
25. Rollins, K.M.; Olsen, R.J.; Egbert, J.J.; Jensen, D.H.; Olsen, K.G.; Garrett, B.H. Pile Spacing Effects on Lateral Pile Group Behavior: Load Tests. *J. Geotech. Geoenviron. Eng.* **2006**, *132*, 1262–1271. [[CrossRef](#)]
26. Vesic, A.S. Design of Pile Foundations. In *NCHRP Synthesis of Highway Practice*; Transportation Research Board: Washington, DC, USA, 1977.
27. Garala, T.K.; Madabhushi, G.S.P. Role of Pile Spacing on Dynamic Behavior of Pile Groups in Layered Soils. *J. Geotech. Geoenviron. Eng.* **2021**, *147*, 04021005. [[CrossRef](#)]
28. Khari, M.; Kassim, K.A.; Adnan, A. An Experimental Study on Pile Spacing Effects under Lateral Loading in Sand. *Sci. World J.* **2013**, *2013*, 734292. [[CrossRef](#)]
29. Lin, C.; Wang, G.; Guan, C.; Feng, D.; Zhang, F. Experimental Study on the Shear Characteristics of Different Pile-Soil Interfaces and the Influencing Factors. *Cold Reg. Sci. Technol.* **2023**, *206*, 103739. [[CrossRef](#)]
30. Chen, C.; Yang, Q.; Leng, W.; Dong, J.; Xu, F.; Wei, L.; Ruan, B. Experimental Investigation of the Mechanical Properties of the Sand–Concrete Pile Interface Considering Roughness and Relative Density. *Materials* **2022**, *15*, 4480. [[CrossRef](#)] [[PubMed](#)]
31. Dijkstra, J.; Broere, W.; Heeres, O.M. Numerical Simulation of Pile Installation. *Comput. Geotech.* **2011**, *38*, 612–622. [[CrossRef](#)]
32. Chandrasekaran, S.S.; Boominathan, A.; Dodagoudar, G.R. Group Interaction Effects on Laterally Loaded Piles in Clay. *J. Geotech. Geoenviron. Eng.* **2010**, *136*, 573–582. [[CrossRef](#)]
33. Gavin, K.G.; O’Kelly, B.C. Effect of Friction Fatigue on Pile Capacity in Dense Sand. *J. Geotech. Geoenviron. Eng.* **2007**, *133*, 63–71. [[CrossRef](#)]
34. Ashford, S.A.; Juirnarongrit, T. Evaluation of Pile Diameter Effect on Initial Modulus of Subgrade Reaction. *J. Geotech. Geoenviron. Eng.* **2003**, *129*, 234–242. [[CrossRef](#)]
35. Comodromos, E.M.; Papadopoulou, M.C.; Rentzeperis, I.K. Pile Foundation Analysis and Design Using Experimental Data and 3-D Numerical Analysis. *Comput. Geotech.* **2009**, *36*, 819–836. [[CrossRef](#)]
36. Sun, B.; Jiang, C.; Pang, L.; Liu, P.; Li, X. Effect of the Pile Diameter and Slope on the Undrained Lateral Response of the Large-Diameter Pile. *Comput. Geotech.* **2022**, *152*, 104981. [[CrossRef](#)]
37. Pender, M.J.; Carter, D.P.; Pranjoto, S. Diameter Effects on Pile Head Lateral Stiffness and Site Investigation Requirements for Pile Foundation Design. *J. Earthq. Eng.* **2007**, *11*, 1–12. [[CrossRef](#)]
38. Gil-Martín, L.M.; Fernández-Ruiz, M.A.; Hernández-Montes, E. Effective Moment of Inertia of Reinforced Concrete Piles. *ACI Struct. J.* **2022**, *119*, 167.

39. Zha, J. *Finite Element Analysis of Nonlinear Dynamic Pile-Soil Interaction*; State University of New York at Buffalo: Buffalo, NY, USA, 1996; ISBN 9798684660054.
40. Ukritchon, B.; Faustino, J.C.; Keawsawasvong, S. Numerical Investigations of Pile Load Distribution in Pile Group Foundation Subjected to Vertical Load and Large Moment. *Geomech. Eng.* **2016**, *10*, 577–598. [[CrossRef](#)]
41. Zheng, G.; Peng, S.Y.; Ng, C.W.W.; Diao, Y. Excavation Effects on Pile Behaviour and Capacity. *Can. Geotech. J.* **2012**, *49*, 1347–1356. [[CrossRef](#)]
42. Leung, Y.F.; Klar, A.; Soga, K. Theoretical Study on Pile Length Optimization of Pile Groups and Piled Rafts. *J. Geotech. Geoenviron. Eng.* **2010**, *136*, 319–330. [[CrossRef](#)]
43. Randolph, M.F. Science and Empiricism in Pile Foundation Design. *Géotechnique* **2003**, *53*, 847–875. [[CrossRef](#)]
44. Akl, A.Y.; Mansour, M.H.; Moustafa, H.K. Effect of Changing Configurations and Lengths of Piles on Piled Raft Foundation Behaviour. *Civ. Eng. Urban Plan. Int. J.* **2014**, *1*, 49–65.
45. Long, Y.; Zhibing, X.; Xian, L.; Juntao, N.; Sebastian, R. Application of Super Large and Deep Diameter Assembly Shafts in Soft Soil Layers. In *IOP Conference Series: Earth and Environmental Science*; IOP Publishing: Bristol, UK, 2024; Volume 1333, p. 012053.
46. Rahil, F.H.; Al-Neami, M.A.; Al-Zaho, K.A.N. Effect of Relative Density on Behavior of Single Pile and Piles Groups Embedded with Different Lengths in Sand. *Eng. Technol. J.* **2016**, *34*, 1206–1215.

Disclaimer/Publisher's Note: The statements, opinions and data contained in all publications are solely those of the individual author(s) and contributor(s) and not of MDPI and/or the editor(s). MDPI and/or the editor(s) disclaim responsibility for any injury to people or property resulting from any ideas, methods, instructions or products referred to in the content.